Article N° 503
Contribution C.O.B.N° 689

35. THOLEIITES, BASALTIC ANDESITES, AND ANDESITES FROM LEG 60 SITES: GEOCHEMISTRY, MINERALOGY, AND LOW PARTITION COEFFICIENT ELEMENTS[1]

H. Bougault,[2] R. C. Maury,[3] M. El Azzouzi,[3] J.-L. Joron,[4] J. Cotten,[3] and M. Treuil[4]

ABSTRACT

This chapter presents major oxide and trace element determinations of igneous whole-rock compositions from sites drilled during Leg 60 and electron microprobe mineral and glass analyses of samples from Sites 454 and 458. Interarc basin basalts from the Mariana Trough (Sites 454 and 456) are similar in all respects to depleted mid-ocean ridge basalts. Basaltic andesites and andesites from Site 458 (Mariana fore-arc region) are more depleted than mid-ocean ridge basalts and show different geochemical behavior for Zr-, Hf, and Ti when compared on an extended Coryell-Masuda plot.

INTRODUCTION

Samples recovered during DSDP Leg 60 have been investigated for major element geochemistry, mineralogy, and trace element behavior. Major differences between Sites 454 to 456 (tholeiites) and Sites 458 to 459 (basaltic andesites and andesites) correspond to different geological settings. Sites 454 and 456 are located in the Mariana Trough, an interarc basin currently spreading between the Mariana arc and West Mariana Ridge. The basalts are Pliocene and Pleistocene in age. At Sites 458 and 459 we reached lower Oligocene to upper Eocene basement in the fore-arc region of the Mariana arc. The setting and lithologic character of the igneous recovery are described in detail in the site reports of this volume.

THOLEIITES FROM SITE 454

Chemical Composition (major elements)

Five magmatic units were distinguished by the shipboard party at Site 454. In the present chapter, Unit I (massive aphyric basalts) is represented by three samples: 454-5-1, 454-5-3, and 454-5-4; Unit II (fragments of medium-grained basalt) by Sample 454-6,CC; Unit III (thin pillow basalt layers) by Samples 454-8-1 and 454-10-1; Unit IV (massive basalt flows) by Samples 454-11-1, 454-11-2, and 454-12-1; and Unit V (pillow fragments) by Sample 454-16-1. All these lavas are aphyric (with the exception of sample 454-5-4), and their composition is representative of magmatic liquids.

The analyses and C.I.P.W. norms given in Table 1 show a relatively narrow range of composition, all the lavas from Hole 454 being clearly basaltic. Calculating their norms with the assumption that Fe_2O_3 = 1.50%, they are either olivine-hypersthene normative (5 samples) or hypersthene-quartz normative (3 samples). The presence of an important percentage of normative quartz in the case of Sample 454-10-1 seems to be due to an analytical underestimation of Na_2O and that of normative nepheline in Sample 454-5-3 to overestimation of CaO. The porphyritic Sample 454-5-4, which contains several olivine phenocrysts, is noticeably enriched in MgO and depleted in SiO_2 and Al_2O_3 with respect to the other samples. Apart from these variations, the silica-saturated or oversaturated norms, the low amounts of K_2O (0.09–0.48%), the TiO_2 values close to 1%, and the variation of FeO/MgO versus SiO_2 indicate that the lavas from Hole 454 have clearly a tholeiitic character and that they are typical of the MORB magmas group on the basis of major element geochemistry.

Mineralogy

From the petrographic point of view, two types of lavas from Site 454 can be distinguished: glassy samples containing only phenocrysts of olivine and minute octahedra of brown spinel (454-8-1, 454-16-1) and medium- to well-crystallized basalts with plagioclase, pyroxene, olivine, and magnetite in the matrix, and occasionally as phenocrysts.

Spinel-Olivine-Glass Tholeiite (Sample 454-8-1)

This sample contains 10% idiomorphic olivine phenocrysts and 0.1% brown spinel octahedra about 10 μm in size, both of them dispersed in brown homogeneous fresh glass. Some olivine phenocrysts contain glassy inclusions up to 200 μm.

The *spinels* (Table 2) are relatively constant in composition, ranging from 43.8 to 50.5% of (Mg, Fe) Cr_2O_4, 41.9 to 47.4% of (Mg, Fe) Al_2O_4, and 6.1 to 9.0% of (Mg, Fe) $Fe^{3+}_2O_4$. Their Mg/Fe^{2+} ratio is close to 2.2 (2.07–2.42); thus magnesiochromite is the most important compositional end member of these spinels. Their frequent occurrence as idiomorphic inclusions in olivine phenocrysts proves that they represent the liquidus phase of the tholeiitic magmas from Site 454.

The *olivine* compositions (Table 3), Fo_{89-91}, are remarkably constant, without any compositional zoning detectable within the limits of precision of the microprobe. The temperatures of possible equilibrium of these compositions with that of the total rock as well as

[1] *Initial Reports of the Deep Sea Drilling Project*, Volume 60.
[2] Centre Océanologique de Bretagne, CNEXO, B.P. 337, 29273 Brest, Cedex, France.
[3] Université de Bretagne Occidentale, 20 avenue Le Gorgeu, 29279 Brest, Cedex, France.
[4] Laboratoire P. Süe, CNRS, CEN Saclay, B.P. N° 2, 91190 Gif-Sur-Yvette, France.

with that of the glassy matrix have been calculated using Leeman and Scheidegger's (1977) method: they vary in a somewhat irregular manner from 1300°C to 1100°C; consequently the olivine phenocrysts cannot be considered entirely as products of equilibrium crystallization of the enclosing lavas.

Glasses. Their compositions and C.I.P.W. norms are given in Table 4. The homogeneity of the glassy matrix is fairly good; its composition is that of a quartz-normative tholeiite and does not differ very much from that of the total rock (with the exception of MgO, depleted in the glass); it is fairly similar to the composition of the most evolved basalts of Hole 454, which can thus be considered as derived from magmas close in composition to Sample 454-8-1 by fractionation of about 10% olivine phenocrysts.

The glassy inclusions in olivine (Table 4, analyses 18–20) show compositional gradients, with systematic increases of SiO_2 and Al_2O_3, and decreases of FeO* and MgO from their cores to their rims; this indicates that at the time of quenching, olivine was still crystallizing at the expense of its glassy inclusions, the composition of which is markedly depleted in MgO.

Plagioclase and Pyroxene-bearing Tholeiite (Sample 454-11-2)

In the matrix of this sample, the plagioclase crystals range in composition from labradorite (An_{67}) to bytownite (An_{75}); a plagioclase phenocryst (400 μm in diameter) shows a normal-type zoning from An_{63} (core) to An_{50} (rim).

Some clinopyroxene analyses are presented in Table 5. In the Ca-Mg-(Fe + Mn) diagram, the phenocrysts lie near the augite/salite boundary, close to the diopside field; the composition of microlites is less calcic and more iron-rich (augite). These pyroxenes have high Al_2O_3 concentrations (4–7%), and moderate TiO_2 (1.2–1.6%), such as many pyroxenes from MORB-type magmas (Muir and Tilley, 1964; Mevel et al., 1979).

BASALTIC ANDESITES AND ANDESITES FROM SITE 458

Lithology

The five lithologic units in Hole 458 are represented in the present chapter by 14 samples: Unit I (glassy to fine-grained pillowed lavas) by Samples 458-28-1, 458-29-2, and 458-30-2; Unit II (massive flows or sills) by Samples 458-32-3, 458-33-2, 458-35-2, and 458-37-2; Unit III (glassy to fine-grained lavas) by Samples 458-39-3 and 458-40-1; Unit IV (glassy to fine-grained, massive to pillowed lavas) by Samples 458-41-1, 458-43-1, and 458-44-1; Unit V (massive fine-grained lava) by Samples 458-47-1 and 458-48-1. The occurrence of a major discontinuity between Units III and IV has been proposed (see site report, this volume) on the basis of abrupt variations of magnetic inclination and rock composition, the plagioclase-free bronzite andesites characteristic of this site occurring only in Units I and III.

Petrographically, three kinds of lavas can be distinguished among the samples available to us: (1) porphyritic basaltic andesites and andesites, with clinopyroxene and/or plagioclase phenocrysts, plagioclase, pyroxene, magnetite, and glass in the matrix (Samples 458-28-1, 458-29-2, 458-30-2, 458-32-3, 458-37-2, 458-48-1); (2) aphyric, predominantly glassy to fairly crystallized basaltic andesites or andesites, with plagioclase, clinopyroxene and magnetite in the matrix (Samples 458-35-2, 458-39-3, 458-40-1, 458-41-1, 458-43-1, 458-47-2; (3) plagioclase-free andesite (Sample 458-44-1) containing bronzite phenocrysts, clinopyroxene microphenocrysts and microlites, and glass.

It is noteworthy that the single bronzite andesite sample found among those available to us does not belong to Units I or III, where such lavas are relatively common, but to Unit IV, which was overlooked initially. Its occurrence undercuts an important argument for the presence of a major discontinuity between Units III and IV—i.e., the restricted occurrence of bronzite andesites in the upper part of the Site 458 igneous pile.

Chemical Composition (Major Elements)

The analyses and norms of 14 samples from Site 458 are presented in Table 6.

1) All these lavas are clearly of orogenic affinities (in contrast to Hole 454). Almost all of them are silica-oversaturated, the amount of normative quartz reaching more than 10%. The TiO_2 percentages are characteristically very low: about 0.3% in the three upper units and 0.5 to 1% in the lower ones. The K_2O values, often higher than 1%, are too high for anorogenic basic tholeiitic magmas; for similar SiO_2 contents, the compositions are very different from that of Hole 454 lavas, which are MORB-type. Lavas from Site 458 can thus be considered mainly aphyric or subaphyric andesitic (*sensu lato*) rocks, a type rare in island arc magmatism.

2) If SiO_2 values are taken into consideration, they define a relatively narrow compositional range (51–56%); following current classifications of calc-alkaline series, lavas with $SiO_2 < 53\%$ can be called basaltic andesites, those with $SiO_2 > 53\%$, andesites.

3) Generally speaking, lavas from the different units are fairly similar; owing to the small number of available samples, it is difficult to distinguish these units one from another on the basis of major element geochemistry. It is noteworthy, however, that the TiO_2 contents of the three upper units are distinctly lower than in lavas of the two others; this chemical difference supports the idea of a major discontinuity between Units III and IV.

4) The plagioclase-free bronzite andesite Sample 458-44-1 appears to be one of the most evolved lavas of the group (SiO_2 = 55.78%), but its chemical composition is in no way unusual and is almost identical to that of some plagioclase-bearing andesites (e.g., Sample 458-33-2).

Mineralogy

Bronzite Andesite (Sample 458-44-1)

A thin section of this rock shows a few phenocrysts of orthopyroxene (< 1%) in a matrix containing 65% brown glass and 35% elongated laths of clinopyroxene.

Some of the latter crystals reach a size of 100 × 25 μm and may be considered microphenocrysts, the smaller ones being microlites. This rock may be considered a member of the boninite group (Kuroda et al., 1978); it differs from the boninites already dredged from the Mariana arc slope (Dietrich et al., 1978) by its lower MgO content and by lack of olivine and clinoenstatite. Representative analyses of pyroxenes and glasses from Sample 458-44-1 are given in Tables 7 and 8; the pyroxenes have also been plotted on the Ca-Mg-(Fe + Mn) diagram in Figure 1.

Bronzite phenocrysts reach in thin section a size of 800 × 400 μm; their orthorhombic symmetry has been confirmed by X-rays. The composition of their cores is close to Wo_3 En_{84} Fs_{13}; their rims may be slightly more iron-rich (Table 7, analyses 26 to 31). They contain significant amounts of Cr_2O_3 (up to 0.7%), and their TiO_2 and Al_2O_3 contents are very small.

Problem of the ferroaugite phenocrysts. In an attempt to measure the transition metals content of the pyroxenes from Sample 458-44-1, 1 gram of these pyroxenes was separated from the total rock by density and magnetic sorting. Thirty grains of dark green clinopyroxene, up to 200 μm in size, were recovered during this operation. Microprobe study proved that they are Ca-Fe-rich clinopyroxenes (Table 7, analyses 31-36). In the pyroxene classification diagram (Fig. 1) most of them lie in the ferroaugite field, near the ferrosilite/hedenbergite-ferrohedenbergite boundary. They contain significant amounts of Na_2O (0.8 to 1%) and MnO (0.7 to 1%) and are poor in TiO_2 and Al_2O_3. Although these crystals have not been observed in thin section and the small available weight of sample precludes further study, contamination of the oxides during sorting seems to be excluded. Furthermore, some Fe-Ca-rich clinopyroxenes, including ferroaugite, have been found *in situ* in the matrix of the sample; boninites contain relatively iron-rich clinopyroxenes (Kuroda et al., 1978). Obviously such a Fe-rich clinopyroxene cannot have crystallized in equilibrium with bronzite; the orthopyroxene-clinopyroxene geothermometry (Wood and Banno, 1973; Wells, 1977) gives unreasonable results (650°C-850°C) for this pair. If the occurrence of Ca-Fe-rich clinopyroxene phenocrysts in other bronzite andesite samples from Site 458 is confirmed, it will be necessary to consider these minerals as coming from a late stage of crystallization of calc-alkaline magmas of the boninite family.

Microphenocrysts and microlites. Their composition is surprisingly variable: extremely magnesian pigeonite (En_{75-78}), augite, ferroaugite, subcalcic augite, and subcalcic ferroaugite have been found (Table 7 and Fig. 1). Strong compositional variations can be observed in individual microphenocrysts. Table 7 (analyses 37-42) presents three examples of these variations: a core of subcalcic ferroaugite with a rim of magnesian pigeonite, a core of magnesian pigeonite with a rim of augite, and a core of ferroaugite with a rim of subcalcic augite. The most calcic microphenocrysts and microlites (augite, ferroaugite) contain very high amounts of alumina, a peculiarity for which we have no explanation at present. Magnesian pigeonite and augite are the most abundant clinopyroxene varieties in the matrix.

The considerable compositional scatter of these pyroxenes is probably a result of their rapid crystallization in a heterogeneous liquid (see the following). Generally, the major trend (Fig. 1) is a progressive increase of Ca and Fe from bronzite phenocrysts to ferroaugite microlites and microphenocrysts, and eventually (at a later stage of magmatic evolution?) to the ferroaugite phenocrysts described earlier. It is compatible with the hypothesis of a progressive separation of bronzite phenocrysts (together with olivine?) from the initial liquid.

Glasses (Table 8). Their composition is dacitic and roughly similar to that of the perlitic dacite of the boninite group described by Kuroda et al., 1978, excepted for their high Al_2O_3 contents (18%), which may represent secondary alteration. The glasses analyzed far from pyroxene microlites or microphenocrysts are fairly identical (Table 8, analyses 51-56). Compositional gradients can be observed in the vicinity of the pyroxenes (Table 8, analyses 55-59): Si and Al increase, Fe, Mg, and Ca

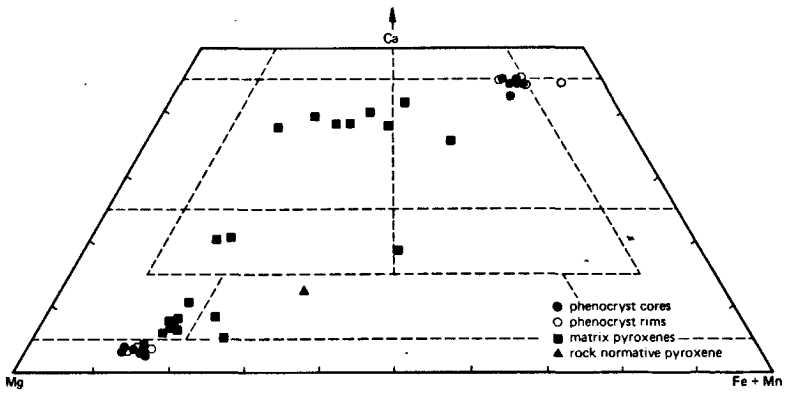

Figure 1. Hole 458: Sample 458-44-1, clinopyroxene composition from bronzite andesite.

decrease toward the pyroxenes, indicating that the rate of crystallization of the pyroxenes was higher than the rate of diffusion in the surrounding liquids; near the pyroxenes, the glasses are thus depleted in the main components of these minerals, as predicted by Albarede and Bottinga (1972).

Plagioclase-bearing Basaltic Andesites and Andesites

Four samples of plagioclase-bearing and orthopyroxene-free andesites, 458-29-2 (Unit I), 458-33-2 and 458-37-2 (Unit II), and 458-47-1 (Unit V), have been investigated by microprobe. They range in composition from relatively basic basaltic andesites (Sample 458-29-2, with SiO_2 = 51.54) to andesites (Sample 454-33-2, with SiO_2 = 55.50) chemically similar to the bronzite andesite sample described earlier.

Pyroxenes (Table 9 and Figure 2). The phenocrysts from Samples 458-29-2, 458-33-2, and 458-37-2 have a restricted range of composition, and most of them lie in the endiopside field near the endiopside/augite boundary. According to the composition of the total rock, the pyroxenes from Sample 458-47-1 are less magnesian and lie in the augite field as do most of the pyroxenes of orogenic magmas series. With respect to the phenocrysts, the microlites are enriched in iron, with or without corresponding decrease of their calcium contents; most of them lie in the augite field. Pyroxenes of endiopsidic compositions have been reported from a number of lavas, most of them located in orogenic series (Konda, 1970; Lowder, 1970; Ewart, 1976); their occurrence in MORB-type lavas seems to be less frequent (Wood et al., 1979a). The pyroxenes from plagioclase-bearing lavas at Site 458 also have very low TiO_2 content (mean value: 0.18%), and their Al_2O_3 percentage is close to 22%. These characteristics are in good agreement with the orogenic affinity of the surrounding lavas; indeed, Le Guen et al. (1979) have shown that pyroxenes from orogenic basic volcanic rocks contain less TiO_2 and Al_2O_3 than those from ocean crust basalts; Nisbet and Pearce's (1977) diagrams also show differences in TiO_2 content between pyroxenes from these two types of lavas.

The compositions of *plagioclases* (Table 10) are labradorite or bytownite. The microlites are usually more calcic (An_{73-70}) than the phenocrysts, the zoning of which is predominantly normal.

CHEMICAL COMPOSITION OF LAVAS FROM OTHER SITES (HOLES 456, 456A, AND 459B)

The analyses of five lavas from Holes 456 and 456A and seven from Hole 459B are given in Table 11A. Major element composition of gabbros recovered in Hole 453 are given in Table 11B.

Lavas from Holes 456A and 456 can be classified either as aphyric basalts with olivine, pyroxene, plagioclase, magnetite, and glass in the matrix (Samples 456A-12-1 and 456-18-1) or as basalts containing some plagioclase phenocrysts, the matrix remaining identical to the former (Samples 456A-14-1, 456-16-2, and 456-19-1). All of these lavas are olivine-hypersthene normative, low in K_2O (<0.4%), and moderately low in TiO_2 (1.1–1.2%). Their similarities with Hole 454 lavas are striking, and they can be related to a MORB-type magmatism.

Lavas from Hole 459B contain plagioclase, olivine, pyroxene, magnetite, and glass in their matrix; they are either aphyric (Samples 459B-60-2, 459B-61-2, 459B-66-2, and 459B-72-1) or porphyritic with plagioclase, clinopyroxene, and olivine phenocrysts (Samples 459B-60-1, 459B-69-1, and 459B-73-2). All of them are quartz-normative, low in TiO_2 (0.7–1.1%), and have a composition similar to that of basaltic andesites and andesites from Site 458 (orogenic magma type).

LOW PARTITION COEFFICIENT ELEMENT: Nb/Ta, Zr/Hf, AND Y/Tb RATIOS

Concentrations of these elements related to the first (Ti, V), second (Y, Zr, Nb), and third transition series (rare earths: La, Ce, Eu, Tb, Hf, Ta) plus Th are given in Tables 12 to 16. Because of the similarities of their

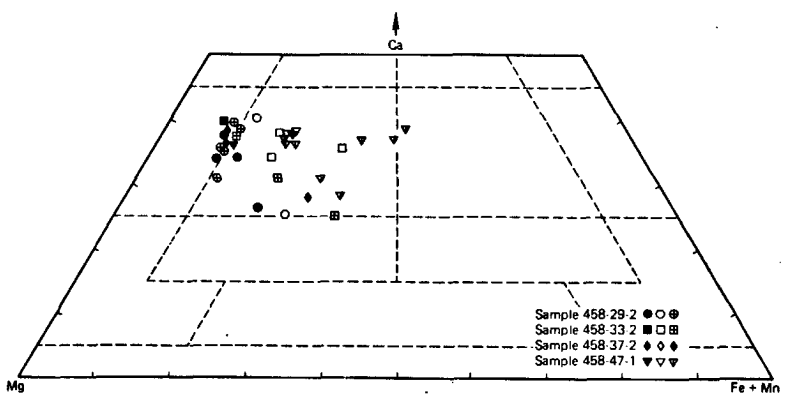

Figure 2. Hole 458: Clinopyroxene composition from lavas. (Black symbols = cores of phenocrysts, open symbols = rims of phenocrysts, symbols with crosses or lines = matrix.)

chemical and physical properties, the elements of the pairs Y-Tb (group IIIA), Zr-Hf (group IVA), and Nb-Ta (group VA) do not fractionate or fractionate very little with respect to each other during magmatic processes. This has been shown to be the case for oceanic tholeiites (Bougault et al., 1979). We shall first, then, examine the behavior of these three pairs of elements according to the two main groups of samples recovered, respectively, at Sites 454 and 456 (tholeiites) on the one hand and 458 and 459 on the other (basaltic andesites and andesites).

Y is plotted versus Tb in Figure 3. As expected, there is a very good correlation between both elements; the data plots near a straight line passing through the origin. The Y/Tb ratio observed in abyssal tholeiites (Bougault et al., 1979) is between 40 and 50, close to the chondritic ratio of 46, taking 2.16 ppm for Y and 0.047 ppm for Tb as average values in chondrites. The ratio defined by the line in Figure 3, about 50, is in the upper range of Y/Tb ratios observed for oceanic tholeiites. We note that there is no significant difference between the two groups of samples at Sites 454 and 456 on the one hand and 458 and 459 on the other.

The plot Hf-Zr is presented in Figure 4. It is also represented by a straight line passing through the origin; the ratio Zr/Hf is 40; this ratio, together with the dispersion of points around the line, is also the same as for oceanic tholeiites—the chondrite ratio. Again, there is no significant difference between Holes 454 and 456 and 458 and 459.

Nb and Ta are plotted in Figure 5. The cross represents the reproducibility of measurements, which is not in the confidence range of absolute values. It seems that the Nb/Ta ratio presents a slight difference between Holes 454 and 456 and 458 and 459. Although the average ratio is higher than the ratio observed in oceanic tholeiites (18), the difference is probably not analytically different, given the precision of the measurements. In addition to the reproducibility of measurements themselves, the absolute concentration in Nb cannot be specified with a precision better than 1 ppm. Thus if Nb concentrations have been overestimated by 1 ppm, the corrected Nb/Ta ratio would correspond to the ratio already observed in oceanic rocks. This is highly probable, especially if we take into account the results obtained for the two other pairs, Zr-Hf and Y-Tb, which have ratios identical to oceanic basalts.

In spite of the Nb/Ta ratio, which has to be interpreted with analytical precision in mind, we can affirm that the three pairs of elements Nb-Ta, Zr-Hf, and Y-Tb present the ratios observed in oceanic rocks and that there are no significant differences between the tholeiites and the basaltic andesites and andesites.

Behavior of Hygromagmaphile Elements: The Use of an Extended Coryell-Masuda Plot

The adjective "hygromagmaphile" was first introduced by Treuil (1973) to emphasize that the behavior of low partition coefficient elements is not a question only of incompatibility in a crystal structure (the notion of L.I.L. elements) but also of affinity for the liquid. Taking both notions into consideration it has been shown that the low partition coefficient elements can be classified according their "bulk" partition coefficients, at least as far as oceanic tholeiites are concerned (Bougault et al., 1979). Recently, Sun et al. (in press) and Wood et al. (1979) proposed an extension of the plot of Coryell and Masuda (Masuda, 1962; Coryell et al., 1963) including other elements besides rare earths. It can be shown that not all elements can be included in such a plot, but only lithophile and hygromagmaphile elements (Bougault et al, in preparation). The big difficulty in making such an extended Coryell-Masuda plot is the knowledge of chondritic average concentrations for elements such as Th, Ta, Nb, Zr, and Hf. We have deter-

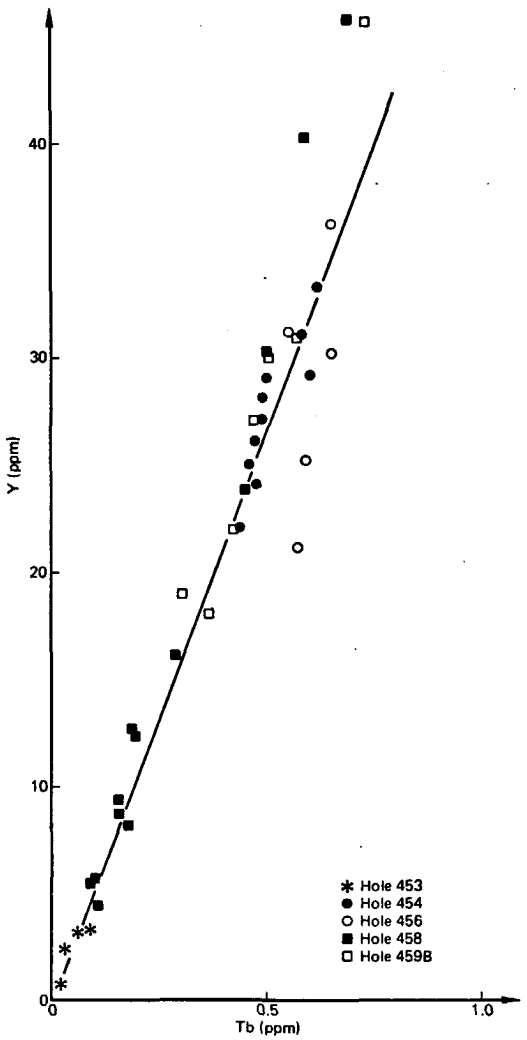

Figure 3. Y versus Tb, all samples.

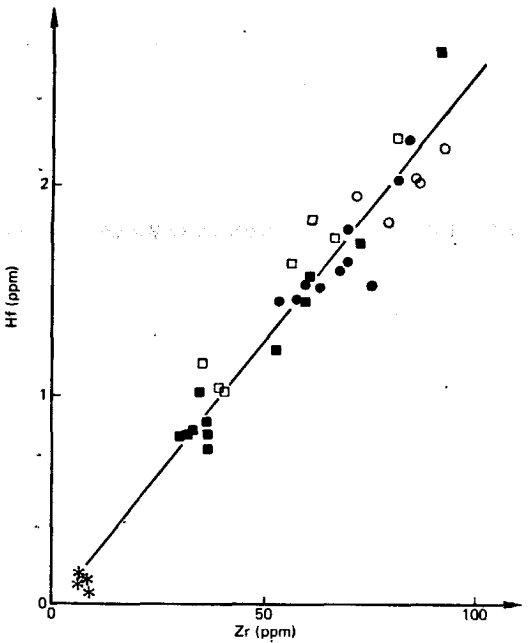

Figure 4. Zr versus Hf. (Symbols same as in Fig. 3.)

mined theoretical chondritic concentrations through comparative geochemistry of several oceanic basalts (Table 17) and the precise locations where these elements should be plotted with respect to the rare earths. These locations confirm the previous classification of these elements comparative to rare earths (Bougault et al., 1979). From a theoretical point of view we propose the following relationship to account for both the incompatible and hygromagmaphile character of these elements:

$$\phi = (a \Delta R_i^2 + 1)\frac{n}{R_i},$$

where R_i is the ionic radius of the low partition coefficient element, n its charge, and ΔR_i the difference between the ionic radius of the element and the major element for which it substitutes in the crystal structure. The parameter a represents the relative weight of the incompatibility and the hygromagmaphile character. This relationship allows us to place the elements Th, Ta, Nb, Zr, Hf, Ti, and Y in exactly the same position as they occupy in the comparative geochemistry (Bougault et al., in preparation). Thus rather than present a Coryell-Masuda plot based on atomic numbers (which is somewhat difficult for non-rare-earth elements), the extended Coryell-Masuda plots in the present chapter are based on the parameter ϕ plotted against the abscissa. An example is given in Figure 6 for Mid-Atlantic Ridge basalts, 45°N, FAMOUS area and Leg 37, and 22°N (Leg 45). On this figure can be seen the difference in

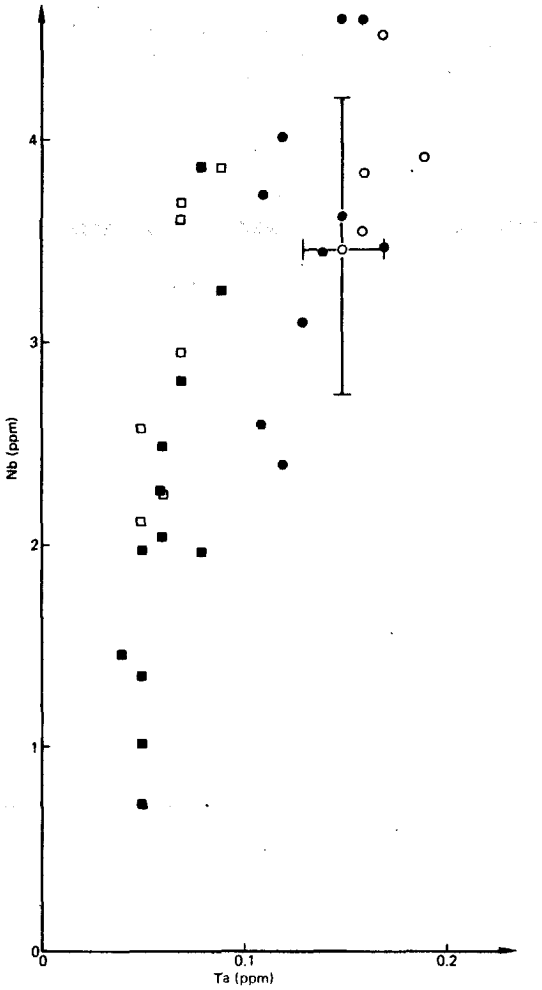

Figure 5. Nb versus Ta. (Symbols same as in Fig. 3.)

Ta/La ratio beween the FAMOUS area (37°N and 45°N on the one hand and 22°N on the other, a difference described elsewhere by Bougault et al. (in preparation).

The extended Coryell-Masuda plot for Sites 454 and 456 is presented in Figure 7. These plots are very similar to mid-ocean ridge tholeiites with flat to light rare-earth-depleted patterns. They resemble what have been called normal or "depleted" tholeiites, such as 22°N samples (Fig. 6). Samples from Sites 454 and 456 show the same "Ta, Nb anomaly"[5] as 22°N samples (Fig. 6).

[5] "Ta, Nb anomaly" means that Ta and Nb normalized values are different (and lower) than the La normalized values. It has been shown that transitional to alkalic affinity basalts have the same Ta, Nb, and La normalized values (Fig. 6); this is not the case for 22°N samples. The notion of "Ta, Nb anomaly" corresponds to the two different La/Ta ratios found in the FAMOUS area at 30°N and at 22°N (Bougault et al., 1978).

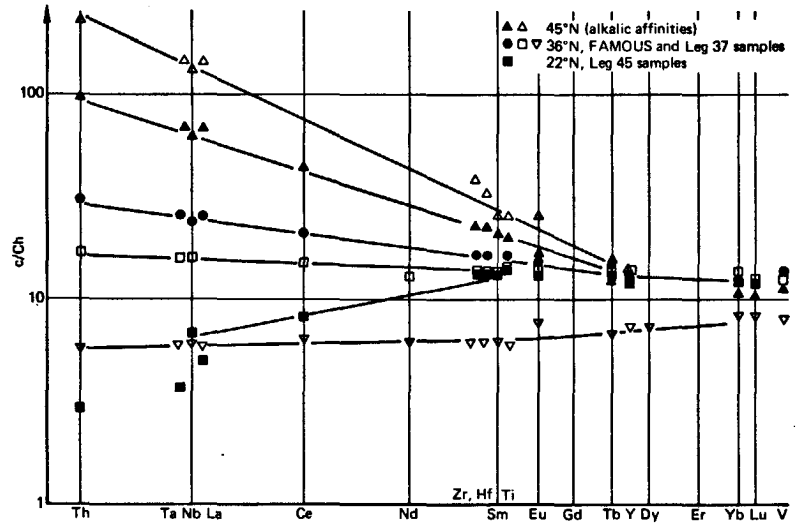

Figure 6. North Atlantic: Examples of normalized chrondrite abundances.

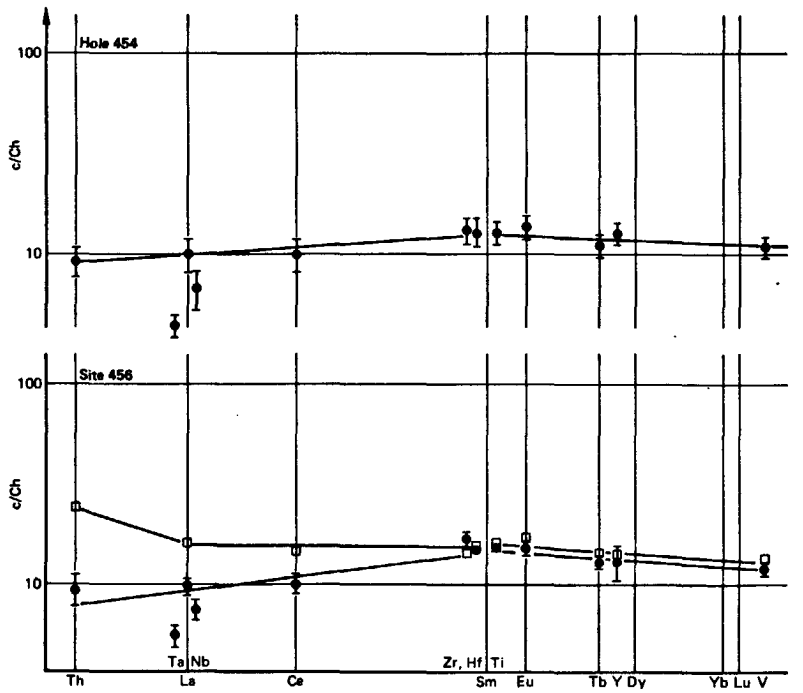

Figure 7. Normalized chondrite abundances for Hole 454 and Site 456. For Hole 454 and Site 456 the limits corresponding to dots are related to the range of variation in the hole or site. For Hole 456A, Sample 456A-12-1, 62–64 cm (open squares) is outside the limits.

Figure 8 shows the extended Coryell-Masuda plot for Sites 458 and 459. On the basis of these patterns, Hole 458 samples can be divided into two groups: (1) samples from Cores 28 to 40, plus Samples 458-44-1 and 458-54-58 (boninite affinity), and (2) others. Group 1 presents two characteristic features: low rare earth content and Zr, Hf, and Ti anomalies compared to oceanic tholeiites. These anomalies are characterized by higher chondrite normalized ratios compared to adjacent rare earths (Eu, Tb); in addition there is fractionation of Zr, and Hf with respect to Ti. For comparison, the data of Dietrich et al. (1978) from the Marianas region are plotted in Figure 9. The samples of dredges 1398 and 1404 have characteristic patterns of tholeiites. This is obviously not the case for sample of dredge 1402, which has shoshonitic affinities, and probably not the case for basalts of 1402, which present a fractionation of heavy rare earths. The boninite type rocks of dredge 1403 show similar features with Group 1 in Hole 458: low abundances of rare earths and Zr-Ti fractionation. In addition, in both cases V does not plot on the rare earth pattern. Whether a similar phenomenon occurs among Leg 60 samples needs to be confirmed by analysis of heavy rare earth elements. In the lower middle part of the diagram, from Zr to Y, the points are linked by a continuous line to emphasize the atypical behavior of these elements at Sites 458 and 459 samples compared with the typical behavior of tholeiites, which should be represented by the discontinuous line (rare earth curve).

Considering Group 2, those samples of Hole 458 with higher rare earth abundances have less, even negligible, fractionation of Zr and Hf with respect to Ti, but the chondrite normalized abundances of these three elements are still higher than those of Eu and Tb. Although to a lesser degree, the same feature is observed among Hole 459B samples. All samples from Sites 458 and 459 show a higher Y/Tb ratio than chondrites.

All samples in Group 1 in Hole 458 are glassy or aphyric and may be considered to represent liquid compositions. The difference in the behavior of hygromagmaphile elements between these rocks and the tholeiites at Sites 454 and 456 is probably due to major differences both in the initial solid materials and in the manner of melting.

From the figures presented, it is easy to see that the diagram Zr, Ti, Y proposed by Pearce and Cann (1973) distinguishes no significant differences among oceanic tholeiites. For oceanic tholeiites, Zr and Ti do not fractionate with respect to each other (Bougault et al., 1978), and the Pearce-Cann diagram is limited to the fractionation of Zr and Ti with respect to Y. From the position of these elements in the extended Coryell-Masuda plot it is clear that the fractionation is the same as that of Sm with respect to Tb. We know that such

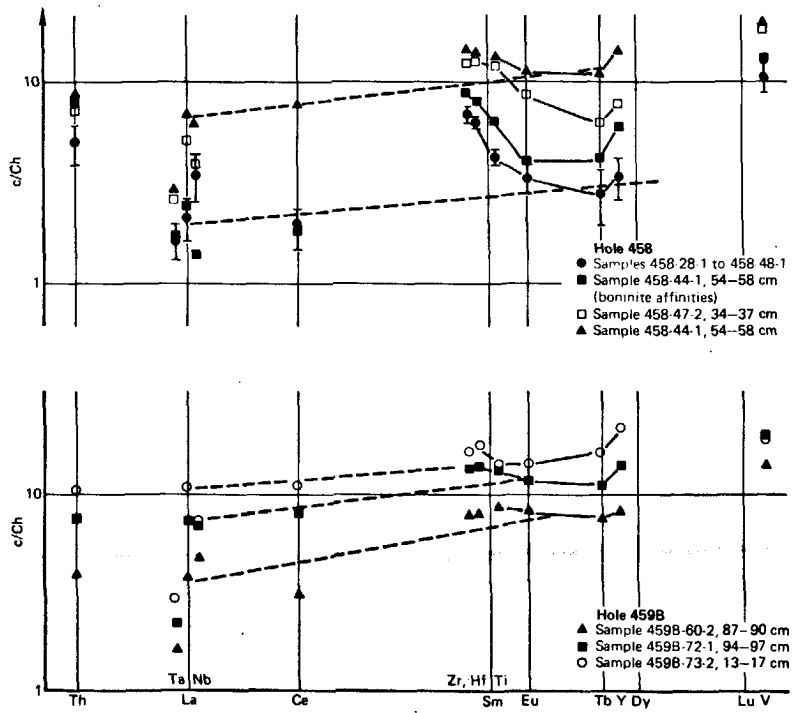

Figure 8. Normalized chondrite abundances for Holes 458 and 459B.

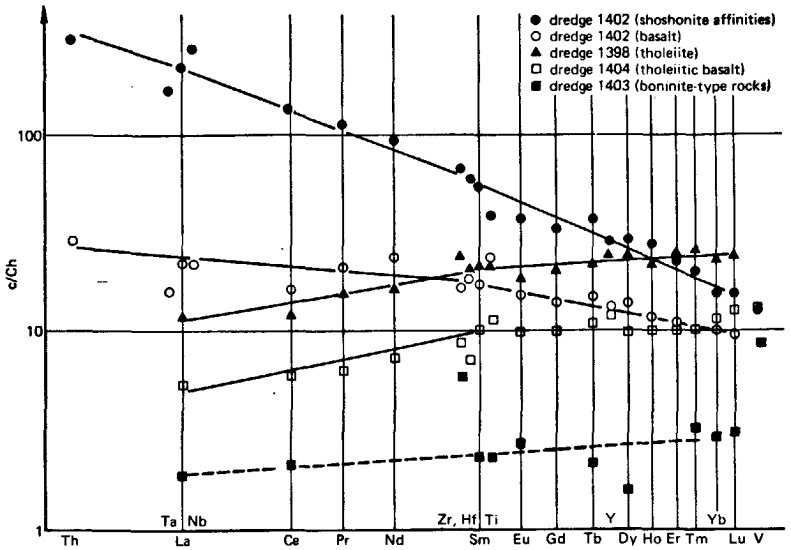

Figure 9. Normalized chondrite abundances from Dietrich et al. (1978).

fractionation is very slight among oceanic tholeiites. By contrast, the Pearce-Cann diagram would show significant differences between Site 458 samples and oceanic tholeiites because of the fractionation of Zr, Ti, and Y in these rocks. Nevertheless we prefer to use the proposed extended Coryell-Masuda plot, which emphasizes the same features but at the same time allows a comparison of several hygromagmaphile elements.

CONCLUSIONS

Major element composition and mineralogy define samples recovered at Sites 454 and 456 as oceanic tholeiites. The extended Coryell-Masuda plots, including within rare earths other low partition coefficient elements, correspond to typical light-rare-earth-depleted tholeiites with a La/Ta ratio about 20 (this ratio is about 9 in tholeiites which have flat- or light-rare-earth-enriched patterns).

The samples recovered at Sites 458 and 459 are basaltic andesites or andesites, based on major element compositions and mineralogy. The bronzite andesite Sample 458-44-1 may be considered as a member of the boninite group; it shows a very complex pyroxene mineralogy (bronzite and ferro-augite phenocrysts and wide compositional range in the matrix). The extended Coryell-Masuda plots show three major differences between these rocks and tholeiites: The absolute abundances of rare earths and other low partition coefficient elements are lower than in tholeiites, the Zr-Hf pair does not plot on the line defined by rare earths, and fractionation exists with respect to Ti.

REFERENCES

Albarede, F., and Bottinga, Y., 1972. Kinetic disequilibrium in trace element partitioning between phenocrysts and host lava. *Geochim. Cosmochim. Acta*, 36:141-156.

Bougault, H., Joron, J. L., and Treuil, M., 1979. Alteration, fractional crystallization, partial melting, mantle properties from trace elements in basalts recovered in the North Atlantic. *Maurice Ewing Series, Vol. 2 (A.G.U.), Deep Drilling Results in the Atlantic ocean;* Ocean Crust.

Bougault, H., Treuil, M., and Joron, J. L., 1978. Trace elements in basalts from 23°N and 36°N in the Atlantic Ocean: fractional crystallization, partial melting, and heterogeneity of the upper mantle. *In* Melson, W. G., Rabinowitz, P. D., et al., *Init. Repts. DSDP*, 45: Washington (U.S. Govt. Printing Office), 493-506.

Bougault, H., Treuil, M., and Joron, J. L., in preparation. Comparative geochemistry of transition elements in oceanic basalts.

Coryell, C. D., Chase, J. W., and Winchester, J. W., 1963. A procedure for geochemical interpretation of terrestrial rare earth abundance patterns. *J. Geophys. Res.*, 68:559-566.

Dietrich, V., Eimmerman, R., Oberhansli, R., et al., 1978. Geochemistry of basaltic and Gabbroic rocks from the West Mariana basin and the Mariana trench. *Earth Planet. Sci. Lett.*, 39:127-144.

Ewart, A., 1976. Mineralogy and chemistry of modern orogenic lavas—some statistics and implications. *Earth Planet. Sci. Lett.*, 31: 417-432.

Konda, T., 1970. Endiopside in the calcalkaline basalt in the Ryozen area. *J. Geol. Soc. Jpn.*, 76:7-12. (In Japanese)

Kuroda, N., Shiraki, K., and Urano, H., 1978. Boninite as a possible calc-alkalic primary magma. *Proc. Tokyo Conf.*, pp. 280-281.

Leeman, W. P., and Scheidegger, K. F., 1977. Olivine/liquid distribution coefficients as a test for crystal liquid equilibrium. *Earth Planet. Sci. Lett.*, 35:247-257.

Le Guen de Kerneizon, M., Mascle, A., Maury, R. C., et al., 1979. Les laves de la Désirade (Petites Antilles), témoins d'un magmatisme de marge active; arguments minéralogiques. *Bull. Bur. Rech. Geol. Min.* 4(3/4):285-292.

Lowder, G. G., 1970. The volcanoes and caldera of Talasea, New Britain: Mineralogy. *Contrib. Mineral. Petrol.*, 26:324-340.

Masuda, A., 1962. Regularities in variation of relative abundances of lanthanide elements and an attempt to analyze separation index patterns of some minerals. *J. Earth Sci., Nagoya Univ.*, 10:173-187.

Mevel, C., Ohnenstetter, D., and Ohnenstetter, M., 1979. Mineralogy and petrology of Leg 46 basalts. *In* Dmitriev, L., Heirtzler, J., et al., *Init. Repts. DSDP*, 46: Washington (U.S. Govt. Printing Office), 151-164.

Muir, I. D, and Tilley, C. E., 1964. Basalts from the northern part of the rift zone of the Mid-Atlantic Ridge. *J. Petrol.*, 5:409–434.

Nisbet, E. G., and Pearce, J. A., 1977. Clinopyroxene composition in mafic lavas from different tectonic settings. *Contrib. Mineral. Petrol.*, 63:149–160.

Pearce, J. A., and Cann, J. R., 1973. Tectonic setting of basic volcanic rocks determined using trace element analyses. *Earth Planet. Sci. Lett.*, 19:290–300.

Sun, S. S., Nesbitt, R. W., and Sharaskin, A. Y., in press. Geochemical characteristics of mid-ocean ridge basalts. E.P.S.L.

Treuil, M., 1973. Critères pétrologiques, géochimiques et structuraux de la génèse et de la différenciation des magmas basaltiques; exemple de l'Afar [Thèse de doctorat d'Etat]. Orléans.

Wells, P. R. A., 1977. Pyroxene thermometry in simple and complex systems. *Contrib. Mineral. Petrol.*, 62:129–139.

Wood, A., Tarney, J., Varet, J., et al., 1979b. Geochemistry of basalts drilled in the North Atlantic by IPOD Leg 49: Implications for mantle heterogeneity. *Earth Planet. Sci. Lett.*, 42:77–97.

Wood, B. J., and Banno, S., 1973. Garnet-orthopyroxene and orthopyroxene-clinopyroxene relationships in simple and complex systems. *Contrib. Mineral. Petrol.*, 42:109–124.

Wood, D. A., Varet, J., Bougault, H., et al., 1979a. The petrology, geochemistry and mineralogy of North Atlantic basalts. A discussion based on IPOD Leg 49. *In* Luyendyk, B. P., Cann, J. R., et al., *Init. Repts. DSDP*, 49: Washington (U.S. Govt. Printing Office), 597–655.

Table 1. Hole 454: Major elements and C.I.P.W. norms.

	Sample 454-5-1, 38-40 cm[a]	Sample 454-5-3, 52-54 cm[a]	Sample 454-5-4, 50-52 cm[b]	Sample 454-6,CC, 16-18 cm[a]	Sample 454-8-1, 35-37 cm	Sample 454-10-1, 58-60 cm[a]	Sample 454-11-1, 78-80 cm[a]	Sample 454-11-2, 41-43 cm[a]	Sample 454-12-1, 88-90 cm[a]	Sample 454-14-1, 12-14 cm	Sample 454-16-1 138-141 cm
SiO_2	50.96	48.92	48.24	50.72	49.84	52.38	51.26	51.15	51.90	50.60	50.59
Al_2O_3	17.59	16.38	14.07	17.07	15.62	16.97	15.91	15.43	17.36	15.35	15.61
FeO											
Fe_2O_3	8.12	7.70	8.74	8.35	8.77	8.28	8.28	9.30	8.16	8.98	9.46
MnO	0.125	0.112	0.116	0.116	0.114	0.138	0.125	0.15	0.120	0.148	0.157
MgO	6.20	7.27	14.05	8.24	10.71	6.75	7.53	7.28	6.71	7.23	9.48
CaO	13.45	15.99	10.59	12.46	11.81	12.10	12.04	11.46	11.87	11.16	10.45
Na_2O	2.91	2.41	2.04	2.50	2.19	0.52	2.38	2.32	2.41	2.69	2.48
K_2O	0.32	0.16	0.14	0.09	0.26	0.39	0.25	0.33	0.37	0.56	0.48
TiO_2	1.00	0.96	0.83	0.94	0.89	1.00	0.96	1.06	1.02	1.23	1.11
P_2O_5	0.13	0.13	0.11	0.11	0.13	0.14	0.13	0.14	0.14	0.16	0.14
Total	100.81	100.03	98.93	100.60	100.28	98.67	98.87	98.62	100.06	98.11	99.96
Loss on Ignition 110°C	1.09	0.99	0.95	1.2	0.23	0.23			1.53		0.54
Loss on Ignition 1050°C	1.27	3.95	1.5		0.98	1.98			1.56		0.63
Q						12.15	1.91	2.26	2.54		
or	1.89	0.95	0.84	0.53	1.54	2.35	1.47	1.99	2.20		2.86
ab	24.58	16.39	17.57	21.16	18.60	4.49	20.04	20.05	20.51		21.15
an	33.94	33.60	29.35	35.12	32.15	43.70	36.12	31.39	35.68		30.30
ne		2.63									
di wo	13.29	18.92	9.77	10.86	10.77	6.94	9.02	10.76	9.45		9.79
di en	8.15	12.38	6.99	7.09	7.32	4.32	5.80	6.51	5.93		5.69
di fs	4.38	5.22	1.91	3.02	2.61	2.20	2.62	3.66	2.95		2.50
en	3.11		9.32	10.46	10.07	12.83	12.91	12.01	10.88		13.07
fs	1.67		2.55	4.46	3.59	6.53	5.83	6.75	5.41		5.75
fo	2.91	4.08	13.53	2.10	6.57						3.53
fa	1.72	1.90	4.08	0.99	2.58						1.71
mt	2.17	2.19	2.21	2.18	2.18	2.22	2.17	2.22	2.19		2.19
il	1.90	1.83	1.61	1.79	1.70	1.94	1.82	2.06	1.95		2.13
ap	0.31	0.31	0.37	0.26	0.31	0.34	0.31	0.34	0.33		0.33
S.I.	36.75	43.07	58.02	44.62	50.61	44.28	42.68	39.46	39.58		44.90
D.I.	26.46	19.57	18.41	21.69	20.14	18.99	23.42	24.31	25.25		24.01

Note: The norms are calculated on the basis of Fe_2O_3 = 1.5% (total Fe analysis is given as Fe_2O_3).
[a] Subaphyric basalts: glass, olivine, pyroxene, plagioclase, and magnetite are present in the matrix.
[b] Porphyritic: olivine, plagioclase, and pyroxene are present as phenocrysts. The matrix is olivine, plagioclase, pyroxene, magnetite, and glass.

Table 2. Hole 454: Sample 454-8-1, spinel analyses normalized to 32 oxygens.

Analysis	1	2	3	4	5
SiO_2	0.09	0.00	0.10	0.10	0.34
TiO_2	0.48	0.42	0.40	0.41	0.46
Al_2O_3	26.56	25.58	25.62	26.92	23.05
Cr_2O_3	36.76	39.29	39.77	39.25	41.47
Fe_2O_3	7.93	6.97	5.91	5.42	6.59
FeO	12.27	12.71	13.06	11.91	12.58
MnO	0.18	0.15	0.14	0.04	0.07
MgO	15.75	15.50	15.16	16.15	15.14
CaO	0.00	0.14	0.01	0.00	0.08
Na_2O	0.04	0.00	0.00	0.00	0.00
K_2O	0.00	0.00	0.00	0.00	0.01
Total	100.06	100.76	100.17	100.30	99.79
Si	0.022	0.000	0.025	0.023	0.083
Ti	0.086	0.075	0.072	0.073	0.084
Al	7.456	7.181	7.232	7.506	6.586
Cr	6.923	7.401	7.531	7.361	7.949
Fe^{3+}	1.422	1.250	1.065	0.964	1.202
Fe^{2+}	2.445	2.532	2.617	2.356	2.551
Mn	0.037	0.031	0.029	0.009	0.015
Mg	5.590	5.503	5.413	5.698	5.471
Ca	0.000	0.036	0.003	0.000	0.021
Na	0.020	0.000	0.000	0.000	0.000
K	0.000	0.000	0.000	0.000	0.002

Note: Fe^{2+} and Fe^{3+} estimated from stoichiometry. All microprobe analyses reported in this chapter were performed with a CAMEBAX automatized microprobe (working conditions: H15kV, 10–12 nA, counting time: 6 s).

Table 3. Hole 454: Sample 454-8-1, olivine analyses normalized to 4 oxygens.

Analysis	6	7	8	9	10	11	12	13
SiO_2	40.54	41.04	40.63	41.16	40.64	41.04	40.64	40.81
TiO_2	0.01	0.00	0.00	0.00	0.00	0.00	0.01	0.01
Al_2O_3	0.03	0.04	0.10	0.00	0.08	0.04	0.02	0.01
Cr_2O_3	0.00	0.00	0.00	0.00	0.00	0.08	0.00	0.06
FeO*	9.73	9.70	10.20	10.19	10.48	9.70	8.95	9.29
MnO	0.03	0.26	0.18	0.14	0.11	0.27	0.16	0.03
MgO	48.49	48.89	48.83	48.59	49.11	49.73	49.63	48.90
CaO	0.19	0.32	0.30	0.27	0.26	0.25	0.27	0.35
Na_2O	0.02	0.00	0.01	0.00	0.01	0.01	0.01	0.00
K_2O	0.00	0.00	0.00	0.00	0.01	0.03	0.01	0.00
Total	99.04	100.25	100.25	100.35	100.70	101.15	99.70	99.46
Si	1.002	1.002	0.995	1.006	0.992	0.995	0.996	1.003
Ti	0.000	0.000	0.000	0.000	0.000	0.000	0.000	0.000
Al	0.001	0.001	0.003	0.000	0.002	0.001	0.001	0.000
Cr	0.000	0.000	0.000	0.000	0.000	0.002	0.000	0.001
Fe	0.201	0.198	0.209	0.208	0.214	0.197	0.184	0.191
Mn	0.001	0.006	0.004	0.003	0.002	0.006	0.003	0.001
Mg	1.786	1.780	1.783	1.770	1.788	1.797	1.812	1.791
Ca	0.005	0.008	0.008	0.007	0.007	0.006	0.007	0.009
Na	0.001	0.000	0.001	0.000	0.000	0.001	0.000	0.000
K	0.000	0.000	0.000	0.000	0.000	0.001	0.000	0.000
Fo %	89.85	89.74	89.34	89.34	89.21	89.88	90.66	90.33

Note: 6: phenocryst (ϕ = 400 μm) core. 7–10: core to rim analyses of a phenocryst about 200 μm large. 11–13: core to rim analyses of a phenocryst about 100 μm large. FeO*: total iron expressed as FeO.

Table 4. Hole 454: Major elements and C.I.P.W. norms of glasses from Sample 454-8-1.

Analysis		14	15	16	17	18	19	20
SiO_2		48.97	49.28	48.92	51.95	50.12	51.03	51.82
TiO_2		0.85	0.97	0.90	0.88	0.98	0.96	0.99
Al_2O_3		16.41	16.52	16.47	18.25	18.23	18.55	19.77
Cr_2O_3		0.04	0.02	0.07	0.00	0.08	0.10	0.00
FeO		7.19	6.93	6.98	6.88	6.36	6.21	5.48
MnO		0.20	0.12	0.05	0.14	0.19	0.10	0.10
MgO		9.35	9.26	9.36	6.81	4.28	3.76	2.72
CaO		13.50	12.99	12.96	9.87	13.35	12.95	13.13
Na_2O		0.86	0.70	0.41	1.85	2.25	2.23	2.71
K_2O		0.19	0.13	0.17	0.24	0.15	0.23	0.30
P_2O_5		0.32	0.39	0.32	0.15	0.29	0.26	0.42
Total		97.88	97.31	96.61	97.02	96.28	96.38	97.44
Q		2.79	5.25	6.00	7.67	4.87	6.84	6.48
or		1.15	0.79	1.04	1.46	0.92	1.41	1.82
ab		7.42	6.08	3.59	16.10	19.75	19.56	23.48
an		41.18	42.64	44.05	41.97	40.69	41.41	41.90
di	wo	10.44	8.71	8.46	3.09	10.89	9.79	9.19
	en	7.07	6.02	5.84	1.98	6.37	5.60	5.12
	fs	2.57	1.99	1.94	0.96	4.00	3.76	3.71
en		16.68	17.64	18.26	15.47	4.69	4.11	1.82
fs		6.07	5.84	6.05	7.04	2.95	2.76	1.32
mt		2.22	2.23	2.25	2.24	2.26	2.26	2.23
il		1.65	1.89	1.77	1.72	1.93	1.89	1.93
ap		0.77	0.95	0.78	0.37	0.71	0.64	1.02
S.I.		52.53	54.03	55.13	42.78	32.35	30.01	24.03
D.I.		11.36	12.11	10.62	25.23	25.54	27.81	31.78

Note: 14–17: glassy matrix. 18–20: glassy inclusions in olivine (18: core; 20: rim).

Table 5. Hole 454: Sample 454-11-2, pyroxene analyses normalized to 8 oxygens.

Analysis	21	22	23	24	25
SiO_2	49.47	49.22	49.46	48.43	50.49
TiO_2	1.30	1.60	1.20	1.73	1.31
Al_2O_3	6.44	7.26	6.25	6.12	4.03
Cr_2O_3	0.00	0.00	0.04	0.16	0.01
FeO*	6.21	6.49	6.54	8.52	12.97
MnO	0.00	0.14	0.13	0.11	0.14
MgO	14.65	13.87	14.24	13.27	15.19
CaO	20.94	20.66	20.37	20.66	14.37
Na_2O	0.27	0.26	0.30	0.31	0.21
K_2O	0.00	0.00	0.00	0.00	0.00
Total	99.28	99.50	98.53	99.31	98.72
Si	1.823	1.813	1.839	1.805	1.893
Ti	0.036	0.044	0.034	0.049	0.037
Al	0.280	0.315	0.274	0.270	0.178
Cr	0.000	0.000	0.001	0.005	0.000
Fe	0.191	0.200	0.203	0.267	0.407
Mn	0.000	0.004	0.004	0.004	0.005
Mg	0.805	0.762	0.789	0.741	0.849
Ca	0.827	0.815	0.811	0.829	0.577
Na	0.019	0.019	0.021	0.022	0.015
K	0.000	0.000	0.000	0.000	0.000
Ca	45.4	45.8	44.9	45.1	31.4
Mg	44.1	42.7	43.6	40.2	46.2
Fe + Mn	10.5	11.5	11.5	14.7	22.4

Note: 21 and 22: cores. 23: rim of a phenocryst. 24 and 25: matrix.

Table 6. Hole 458: Major elements and C.I.P.W. norms.

Sample (interval in cm)	458-28-1, 102-104	458-29-2, 51-54	458-30-2, 32-35	458-32-3, 110-112	458-33-2, 115-117	458-35-2, 95-98	458-37-2, 31-35	458-39-3, 24-27	458-40-1, 116-118	458-41-1, 60-63	458-43-1, 88-92	458-44-1, 54-58	458-47-1, 56-69	458-47-2, 34-47	458-48-1 41-43
SiO_2	52.97	52.55	53.32	55.77	55.50	53.39	53.12	53.58	53.60	55.03	52.62	55.78	51.99	53.86	51.98
Al_2O_3	16.70	16.06	16.30	15.17	14.95	17.66	16.04	17.17	15.77	18.80	16.81	14.89	16.74	15.11	16.56
FeO															
Fe_2O_3	8.89	9.26	9.11	8.44	8.28	8.90	8.78	9.76	10.16	9.98	10.20	10.34	13.47	13.12	13.54
MnO	0.138	0.118	0.117	0.112	0.12	0.105	0.110	0.093	0.108	0.087	0.084	0.156	0.110	0.090	0.093
MgO	6.91	8.62	8.11	5.59	6.65	5.06	6.86	6.23	8.16	1.93	5.14	7.45	5.16	4.78	5.37
CaO	11.73	9.58	9.20	10.81	10.88	9.81	11.28	8.79	7.44	6.34	9.83	8.35	7.35	6.18	6.72
Na_2O	1.93	2.23	2.26	1.94	1.98	2.31	1.98	2.34	2.10	4.34	2.65	2.07	3.00	2.89	3.02
K_2O	0.72	0.98	1.21	0.84	0.73	1.41	1.04	1.30	1.14	1.78	2.46	0.57	0.42	0.76	0.56
TiO_2	0.32	0.32	0.32	0.27	0.29	0.34	0.30	0.35	0.34	1.05	0.55	0.50	1.01	0.92	0.98
P_2O_5	0.04	0.04	0.04	0.07	0.06	0.07	0.07	0.04	0.04	0.26	0.09	0.06	0.14	0.07	0.12
Total	100.35	99.76	99.99	99.01	99.44	99.06	99.58	99.75	98.86	99.60	100.43	100.17	99.36	97.78	98.94
Loss on Ignition 110°C	1.82	2.81	2.91	0.81	0.83	2.29	1.12	3.71	4.09	1.52	2.95	3.01	2.96	4.36	3.18
Loss on Ignition 1050°C	1.30	2.33	2.58	0.77	0.74	1.98	1.34	3.26	3.52	1.81	2.76	3.59	2.37	15.33	2.84
Q	3.83	0.99	2.03	10.58	8.99	4.59	3.82	3.93	4.74	2.89		9.43	3.22		3.01
or	4.27	5.85	7.20	5.05	4.37	8.47	6.22	7.77	6.87	10.65	14.60	3.39	2.53		3.39
ab	16.39	19.05	19.26	16.69	16.96	19.87	16.94	20.03	18.12	37.17	22.51	17.63	25.85		26.13
an	34.92	31.24	31.00	30.72	30.12	34.23	32.18	32.90	30.86	26.90	26.83	29.87	31.55		30.67
ne															
wo	9.70	6.89	6.15	9.75	10.07	6.18	10.00	4.57	2.73	1.35	9.00	4.78	1.94		1.10
di en	5.69	4.25	3.75	5.45	6.02	3.25	5.89	2.49	1.60	0.42	4.48	2.71	0.83		0.48
fs	3.54	2.24	2.05	3.91	3.53	2.74	3.62	1.93	1.00	0.98	4.33	1.87	1.11		0.62
en	11.58	17.43	16.59	8.71	10.75	9.56	11.39	13.21	19.13	4.45	5.17	15.97	12.18		13.20
fs	7.21	9.16	9.07	6.25	6.30	8.07	7.00	10.22	11.98	10.37	5 00	11.06	16.29		16.99
fo											2.25				
fa											2.40				
mt	2.18	2.20	2.19	2.21	2.20	2.21	2.20	2.20	2.22	2.20	2.18	2.19	2.22		2.23
il	0.61	0.61	0.61	0.52	0.56	0.66	0.58	0.67	0.66	2.02	1.05	0.96	1.95		1.90
ap	0.10	0.10	0.10	0.17	0.14	0.17	0.17	0.10	0.62	0.21	0.21	0.14	0.34		0.29
S.I.	39.04	42.50	40.75	34.77	39.27	29.94	28.34	33.24	39.51	11.27	26.34	38.09	24.68		25.30
D.I.	24.48	25.89	28.49	32.32	30.31	32.93	26.98	31.73	29.74	50.71	37.11	30.45	31.60		32.53

Note: Fe_2O_3: total iron expressed as Fe_2O_3.

Table 7. Hole 458: Sample 458-44-1, pyroxene analyses of bronzite andesite normalized to 6 oxygens.

	Phenocrysts											
Analysis	26	27	28	29	30	31	32	33	34	35	36	37
SiO_2	56.37	56.88	56.22	56.70	56.26	56.38	49.63	49.27	49.68	49.20	48.65	46.03
TiO_2	0.08	0.01	0.02	0.05	0.00	0.01	0.35	0.32	0.42	0.29	0.27	0.67
Al_2O_3	0.64	0.63	1.01	1.59	1.92	1.35	1.22	1.32	1.25	1.20	1.29	12.04
Cr_2O_3	0.28	0.52	0.69	0.59	0.54	0.47	0.00	0.00	0.08	0.02	0.00	0.00
FeO*	10.19	8.31	8.40	8.14	8.74	9.19	23.79	23.99	24.24	24.47	26.49	21.26
MnO	0.09	0.13	0.25	0.24	0.25	0.31	0.77	1.02	0.85	0.87	1.04	0.23
MgO	31.76	32.12	31.48	32.49	31.73	31.34	3.94	3.56	33.94	3.39	1.70	11.66
CaO	1.40	1.84	1.84	1.58	1.78	1.99	19.66	19.49	19.24	19.34	19.14	7.46
Na_2O	0.02	0.01	0.04	0.00	0.00	0.01	0.85	0.95	0.81	0.77	1.15	0.78
K_2O	0.00	0.00	0.00	0.00	0.01	0.00	0.02	0.00	0.00	0.00	0.00	0.02
Total	100.83	100.45	99.95	101.38	101.23	101.05	100.23	99.92	99.96	99.55	99.73	100.15
Si	1.969	1.979	1.965	1.953	1.948	1.960	1.973	1.979	1.980	1.972	1.973	1.741
Ti	0.002	0.000	0.001	0.001	0.000	0.000	0.011	0.010	0.012	0.009	0.008	0.019
Al	0.027	0.026	0.042	0.065	0.078	0.055	0.057	0.063	0.059	0.057	0.062	0.537
Cr	0.008	0.014	0.019	0.016	0.015	0.013	0.000	0.000	0.002	0.001	0.000	0.000
Fe	0.298	0.242	0.246	0.235	0.253	0.267	0.791	0.806	0.808	0.820	0.899	0.673
Mn	0.003	0.004	0.007	0.007	0.007	0.006	0.026	0.035	0.029	0.030	0.036	0.007
Mg	1.653	1.666	1.643	1.668	1.637	1.624	0.234	0.213	0.201	0.203	0.103	0.657
Ca	0.052	0.069	0.069	0.058	0.066	0.074	0.837	0.839	0.822	0.830	0.832	0.302
Na	0.001	0.001	0.002	0.000	0.000	0.001	0.066	0.074	0.062	0.060	0.091	0.057
K	0.000	0.000	0.000	0.000	0.001	0.000	0.001	0.000	0.000	0.000	0.000	0.001
Ca	2.600	3.500	3.500	3.000	3.400	3.800	44.300	44.300	44.200	44.100	44.50	18.500
Mg	82.400	84.100	83.600	84.800	83.400	82.300	12.400	11.300	10.800	10.800	5.50	40.000
Fe + Mn	15.000	12.400	12.900	12.200	13.200	13.900	43.300	44.400	45.000	45.00	50.00	41.500

Note: 26 to 36: phenocrysts (> 100 μm) of bronzite (26 to 31) and ferroaugite (32-36). 26 and 27: core; 28-31, core to rim analyses of a 200 μm in diameter crystal; 32-34: cores; 35 and 36: rims. 37-42: 20-50 μm microphenocrysts; 37, 39 and 41: cores; 38, 40, and 42: rims; 43-50: microlites (< 20 μm).

Table 7. (Continued).

Microphenocrysts					Microlites							
38	39	40	41	42	43	44	45	46	47	48	49	50
55.49	55.66	45.05	50.55	53.96	50.10	47.17	46.01	44.15	55.24	55.08	50.44	54.21
0.05	0.09	0.97	0.58	0.16	0.56	0.83	0.78	1.19	0.03	0.07	0.01	0.08
1.13	1.15	10.55	14.55	2.83	5.63	7.90	8.53	10.34	1.14	1.18	1.11	2.58
0.00	0.24	0.00	0.01	0.06	0.07	0.00	0.00	0.00	0.25	0.31	0.09	0.09
10.85	11.57	15.08	15.33	9.96	9.64	13.29	14.39	16.91	11.22	11.06	11.06	14.22
0.31	0.20	0.22	0.21	0.26	0.15	0.30	0.24	0.13	0.16	0.31	0.22	0.28
28.57	28.25	10.44	5.32	22.59	15.90	12.51	11.73	19.89	28.23	27.90	28.59	25.68
3.68	3.43	17.63	10.97	10.01	17.96	17.52	17.37	16.54	3.76	4.11	3.39	4.37
0.03	0.005	0.27	1.13	0.05	0.23	0.31	0.19	0.23	0.02	0.03	0.29	0.07
0.02	0.00	0.00	0.31	0.00	0.00	0.00	0.00	0.02	0.01	0.00	0.00	0.00
100.13	100.64	100.21	98.96	99.87	100.14	99.83	99.24	99.40	100.06	100.05	101.20	101.58
1.967	1.971	1.705	1.873	1.948	1.843	1.774	1.753	1.697	1.964	1.964	1.980	1.931
0.001	0.002	0.028	0.016	0.045	0.016	0.023	0.022	0.034	0.001	0.002	0.000	0.002
0.047	0.048	0.470	0.636	0.120	0.244	0.350	0.383	0.469	0.048	0.050	0.046	0.108
0.007	0.007	0.000	0.000	0.002	0.002	0.000	0.000	0.000	0.007	0.009	0.003	0.003
0.322	0.343	0.477	0.475	0.301	0.297	0.418	0.458	0.544	0.334	0.330	0.324	0.424
0.009	0.006	0.007	0.006	0.008	0.005	0.010	0.008	0.004	0.005	0.009	0.007	0.008
1.509	1.491	0.589	0.294	1.215	0.866	0.701	0.666	0.567	1.496	1.483	1.495	1.364
0.140	0.130	0.715	0.436	0.387	0.708	0.706	0.709	0.681	0.143	0.157	0.127	0.167
0.002	0.004	0.020	0.081	0.004	0.017	0.022	0.014	0.017	0.002	0.002	0.020	0.005
0.001	0.000	0.000	0.015	0.000	0.000	0.000	0.000	0.001	0.000	0.000	0.000	0.000
7.100	6.600	40.000	36.000	20.300	37.700	38.500	38.500	37.900	7.200	7.900	8.500	8.500
76.200	75.700	32.900	24.300	63.600	46.200	38.200	36.200	31.600	75.700	74.900	76.500	69.500
16.700	17.700	27.100	40.700	16.100	16.100	23.300	25.300	30.500	17.100	17.100	17.000	22.000

Table 8. Hole 458: Sample 458-44-1, glass composition of bronzite andesite.

Analysis	51	52	53	54	55	56	57	58	59	60
SiO_2	61.72	61.80	61 30	61 68	60.16	60.30	60 53	61.34	61.14	52 83
TiO_2	0 33	0 31	0 35	0 36	0 28	0 34	0 39	0 37	0 37	0 24
Al_2O_3	18 86	18 36	18 25	18 53	17 75	18 03	18 05	18 12	17 96	3 26
Cr_2O_3	0 00	0 05	0 01	0 00	0 00	0 00	0 14	0 00	0 01	0 16
FeO*	4.26	4 89	4.98	4 43	5 53	5 51	5.29	5.04	4 81	10.97
MnO	0 01	0 15	0 01	0 01	0 04	0 10	0 14	0 00	0 03	0 25
MgO	0.64	0.52	0.86	0.75	1.29	1.02	0.96	0 91	0.82	21.11
CaO	5 24	5 13	5 25	5 19	5 71	5 71	5 52	5.54	5 31	9 82
Na_2O	2.53	2.63	2.53	2.64	2.64	1 93	2.51	2.21	2.65	0 00
K_2O	0.56	0.56	0.54	0.54	0 50	0 58	0 63	0.50	0 59	0 01
P_2O_5	0 11	0 29	0 11	0 20	0 14	0 09	0 11	0 17	0 13	0 00
Total	94 26	94 69	94 19	94 33	94 04	93.61	94.27	94.20	93.82	98.65
Q	33 23	32.83	31 90	32 65	28 01	32 66	29 73	33 49	31 05	
Or	3 50	3 49	3 38	3 38	3 14	3 65	3 95	3 13	3 71	
ab	22.67	23.46	22.68	23.63	23 70	17 41	22.52	19 81	23.85	
an	26 77	24 84	26 84	25.86	29 09	29 58	28 28	27 95	27 13	
co	5 12	5 06	4 48	4 92	3.00	4.33	3 68	4 54	3 86	
en	1 69	1 37	2.27	1 98	3 41	2.71	2.54	2.40	2.17	
fs	3 79	5 32	5.16	4 06	6 44	6 42	5 95	5 22	4 85	
mt	2 30	2.29	2.31	2.30	2.31	2.32	2.31	2.31	2.31	
il	0 66	0 62	0 70	0 72	0 56	0 69	0 79	0 74	0 75	
ap	0.28	0.73	0.28	0 50	0 35	0 23	0 28	0 43	0 33	
S.I.	8 00	5 94	9.64	8.96	12.89	11 16	10 07	10 51	9 21	
D.I.	59.40	59 79	57.97	59 66	54.85	53.73	56 20	56.43	58.61	

Note: 51, 54: glassy matrix. 55–59: glass composition at 25, 20, 15, 10, and 5 μm from a pyroxene microlite (60).

Table 9. Hole 458: Pyroxene analyses from basaltic andesites and andesites. Normalized to 6 oxygens.

Sample	458-29-2					458-33-2					458-37-2					458-47-1				
Analysis	61	62	63	64	65	66	67	68	69	70	71	72	73	74	75	76	77	78	79	80
SiO_2	54 04	54 15	53 31	54 55	53.51	53 90	54 58	54 13	51 30	52.28	54 64	54 70	54 51	54 81	52.63	52.06	52.67	52 73	51 68	49 60
TiO_2	0 17	0 13	0.13	0 05	0.10	0.07	0 02	0 04	0 26	0 16	0 13	0 07	0 00	0 00	0.10	0 32	0 25	0 41	0 35	0 84
Al_2O_3	2 85	2.32	2.17	2.59	3 10	1 69	1 60	2.17	2.81	2.67	2.06	2.06	2.25	1 68	1 93	2.17	1 90	2.03	1 47	2.90
Cr_2O_3	0 31	0 00	0 00	0.60	0.04	0.45	0 26	0 13	0 00	0 00	0 64	0 00	0 34	0.15	0 06	0 00	0 00	0 00	0 03	0 00
FeO*	7 32	11 39	13 77	5 58	6.19	4 89	5.40	6 01	14 80	10 09	5 72	5 56	5 36	5 35	14 34	10 90	10 26	10 66	16 52	15 68
MnO	0 10	0 17	0 26	0 00	0 13	0.08	0.25	0 19	0 30	0 11	0 00	0 08	0 19	0 13	0 45	0 29	0 29	0 25	0 50	0 24
MgO	18 62	19 18	17 79	18 94	17 89	18 32	18 44	18 50	12.99	15 34	18 90	18 45	18 97	18 75	16 37	15 55	15 51	15 16	14 69	11 94
CaO	16 66	12 82	12.28	17 32	19 00	19 56	19 16	18 65	16 85	18 38	18 50	19 02	17 98	18 90	13.71	17 46	18 20	18 37	13 54	17 02
Na_2O	0 08	0 05	0 16	0 20	0 13	0.09	0 14	0 11	0 18	0 15	0 11	0 12	0 11	0 05	1 21	0 23	0 22	0 25	0 18	0 29
K_2O	0 00	0 00	0 00	0 00	0 00	0 00	0 05	0 00	0 00	0 00	0 00	0 00	0 00	0 00	0 00	0 00	0 00	0 00	0 04	0 00
Total	100 15	100 21	99 87	99 83	100 09	99.05	99 90	99 93	99 49	99 18	100 70	100 06	99 71	99 82	100 80	98 98	99 30	99 86	99 00	98 51
Si	1 951	1 968	1 966	1 962	1 940	1 962	1 973	1 961	1 937	1 943	1 955	1 8713	1 966	1 977	1 948	1 944	1 959	1 953	1 963	1 908
Ti	0 005	0 004	0 004	0 001	0.003	0 002	0 001	0 001	0 007	0 005	0 004	0 002	0 000	0 000	0 003	0 009	0 007	0 011	0 010	0 024
Al	0 121	0 100	0 094	0 110	0 967	0 072	0 068	0 091	0 125	0 117	0 087	0 088	0 096	0 072	0 084	0 095	0 083	0 089	0 066	0 131
Cr	0 009	0 000	0 000	0 017	0 001	0 013	0 007	0 004	0 000	0 000	0 018	0 000	0 010	0 004	0 002	0 000	0 000	0 000	0 001	0 000
Fe	0 221	0 346	0 425	0 168	0 188	0 145	0 163	0 182	0 467	0 314	0 173	0 168	0 162	0 161	0 444	0 340	0 319	0 330	0 525	0 005
Mn	0 003	0 005	0 008	0 000	0 004	0 002	0 008	0 006	0 010	0 004	0 000	0 002	0 006	0 004	0 014	0 009	0 009	0 008	0 016	0 008
Mg	1 002	1 040	0 978	1 015	0 967	0 994	0 994	0 999	0 731	0 850	1 008	0 991	1 020	1 008	0 903	0 866	0 860	0 837	0 832	0 685
Ca	0 645	0 499	0 485	0 667	0 738	0 763	0 742	0 724	0 682	0 732	0 709	0 734	0 695	0 731	0 544	0 698	0 725	0 729	0 551	0 702
Na	0 006	0 004	0 012	0 014	0 010	0 007	0 010	0 08	0 013	0 011	0 008	0 009	0 008	0 004	0 087	0 017	0 016	0 018	0 014	0 022
K	0 000	0 000	0 000	0 000	0 000	0 000	0 02	0 000	0 000	0 000	0 000	0 000	0 000	0 000	0 000	0 000	0 000	0 000	0 002	0 000
Ca	34 5	26 4	25.6	36 1	38 9	40 0	38 9	37 9	36 1	38 5	37 5	38 7	36 9	38 3	28 6	36 5	37 9	38 3	28 6	36 9
Mg	53 5	55 0	51.6	54 9	51 0	52.1	52 1	52.3	38 7	44 8	53.4	52.3	54 2	53 0	47 4	45 2	44 9	44 0	43 3	36.1
Fe + Mn	12 0	18.6	22.8	9 1	10 1	7 9	9 0	9 8	25.2	16 7	9 1	9 0	8 9	8 7	24 0	18 3	17.2	17 7	28 1	27.0

Note: Phenocrysts: cores: 61, 62, 66, 67, 68, 71, 72, 76, 77; rims: 63, 69, 70, 73, 78; matrix pyroxenes: 64, 65, 74, 75, 79, 80.

Table 10. Hole 458: Plagioclase analyses.

Sample	458-29-2			458-33-2		458-47-1				
Analysis	81	82	83	84	85	86	87	88	89	90
SiO_2	53 98	52.82	52.48	53.05	54 33	50 29	50 27	53 86	51 64	51.43
TiO_2	0 00	0 00	0 00	0 07	0 04	0 00	0 00	0 01	0 03	0 01
Al_2O_3	29.32	30 59	30 99	29 40	28.64	31 78	31 5	29.52	31 07	31 08
Cr_2O_3	0 00	0 00	0 00	0.00	0 00	0.00	0.09	0.00	0.00	0.00
FeO*	1 24	0 89	0 80	0 76	1 11	0 62	0 61	1 05	0 71	0 93
MnO	0 00	0 00	0 04	0 00	0 02	0 00	0 04	0 00	0 00	0 00
MgO	0 08	0 30	0 22	0 06	0 20	0 24	0 14	0 06	0 14	0 16
CaO	12.31	13 64	13 78	12.14	11 37	14 76	14 91	11 75	14 05	13 98
Na_2O	3 75	3 03	3 17	3.92	4.45	2.38	2.48	4 11	2.86	3.00
K_2O	0 12	0 00	0.05	0.61	0 19	0.04	0 05	0.08	0 03	0 03
Total	100 80	101 27	101 53	99 41	100 35	100 11	100 09	100 44	100 53	100 62
Ca	64.0	71.3	70.4	63 0	57 9	77.2	69.0	60 9	73.0	71 9
Na	35 3	28 7	29.3	36 9	41.0	22.5	30 4	38 5	26.9	28.0
K	0.7	0.0	0.3	0.1	1 1	0.3	0.6	0.6	0.1	0 1

Note: Phenocrysts—cores: 81, 86, 87; rims: 88; matrix plagioclases: 82, 83, 84, 85, 89, 90.

Table 11A. Holes 456A, 456, and 459: Major elements and C.I.P.W. norms of lavas.

Sample (interval in cm)	456A-12-1, 62-64	456A-14-1, 25-27	456-16-2, 98-100	456-18-1, 25-27	456-19-1, 12-15	459B-60-1, 48-51	459B-60-2, 87-90	459B-61-2, 12-16	459B-66-2, 92-95	459B-69-1, 81-84	459B-72-1, 94-97	459B-73-2, 13-17
SiO_2	49.86	50.53	49.50	49.79	50.77	51.04	53.43	53.74	52.06	55.10	54.01	53.28
Al_2O_3	15.68	16.21	15.22	17.02	15.68	17.20	15.42	15.62	16.62	16.77	16.22	17.48
FeO												
Fe_2O_3	10.12	8.91	10.16	9.52	9.84	11.25	10.20	10.35	12.61	9.78	12.03	12.37
MnO	0.158	0.148	0.29	0.166	0.118	0.118	0.136	0.147	0.166	0.110	0.113	0.120
MgO	6.92	7.14	7.45	5.63	6.20	5.06	6.47	6.16	3.86	3.78	3.45	3.83
CaO	11.99	11.86	12.59	12.75	12.40	11.71	10.98	11.03	8.96	9.16	7.75	7.36
Na_2O	2.41	2.67	2.40	2.76	2.60	2.67	2.49	2.49	3.54	3.47	3.49	3.61
K_2O	0.43	0.37	0.04	0.33	0.28	0.45	0.34	0.35	0.66	0.45	1.16	0.42
TiO_2	1.23	1.15	1.19	1.21	1.14	0.74	0.67	0.70	1.07	0.78	1.02	1.05
P_2O_5	0.16	0.13	0.14	0.15	0.13	0.11	0.09	0.09	0.12	0.11	0.14	0.14
Total	98.96	99.12	98.98	99.28	99.16	100.35	100.23	100.68	99.67	99.51	99.38	99.66
Loss on Ignition 110°C	0.71	0.52	1.88	1.56	2.18	1.70	1.17	0.86	1.69	0.80	1.31	3.04
Loss on Ignition 1050°C	0.77	0.50	7.09	1.67	1.45	1.33	1.02	0.54	1.28	0.69	1.25	2.30
Q						0.30	4.36	4.81	0.71	6.60	3.99	3.89
or	2.59	2.22	0.24	1.98	1.78	2.68	2.02	2.07	3.96	2.69	6.97	2.52
ab	20.78	22.95	21.02	23.69	23.65	22.72	21.20	21.10	30.38	29.74	30.02	30.97
an	31.29	31.67	34.07	33.57	31.14	33.83	30.09	30.48	27.92	29.24	25.60	30.69
ne												
wo	11.80	11.38	12.18	12.37	13.68	9.97	10.07	9.92	6.84	6.71	5.25	2.26
di en	6.81	7.02	7.23	6.85	7.92	4.69	5.51	5.29	2.64	3.02	1.97	0.88
fs	4.46	3.71	4.33	5.05	5.13	5.17	4.20	4.31	4.30	3.65	3.37	1.41
en	9.66	9.69	3.46	4.78	3.51	7.99	10.70	10.08	7.11	6.51	6.76	8.79
fs	6.32	5.12	2.07	3.53	2.28	8.80	8.17	8.22	11.60	7.87	11.56	14.03
fo	0.77	0.96	6.31	1.82	3.46							
fa	0.55	0.56	4.16	1.48	2.47							
mt	2.22	2.21	2.25	2.21	2.34	2.19	2.19	2.18	2.21	2.20	2.21	2.21
il	2.38	2.22	2.34	2.33	2.33	1.41	1.28	1.33	2.06	1.50	1.97	2.02
ap	0.39	0.31	0.34	0.36	0.33	0.26	0.21	0.21	0.29	0.26	0.34	0.34
S.I.	36.37	38.91	39.44	32.25	35.10	27.46	34.75	33.36	19.71	22.75	18.12	20.04
D.I.	23.37	25.18	21.26	25.67	25.43	25.70	27.58	27.99	35.05	39.04	40.98	37.38

Table 11B. Hole 453: Major elements (ppm).

Sample (interval in cm)	453-53-3, 44-47	453-53-5, 77-88	453-55-1, 36-48	453-55-4, 118-123
SiO_2	44.64	45.35	45.35	43.60
Al_2O_3	19.86	19.64	19.38	28.99
FeO				
Fe_2O_3	7.36	5.87	5.75	6.32
MnO	0.118	0.101		0.113
MgO	10.91	9.03	8.90	6.64
CaO	16.13	18.25	18.59	13.38
Na_2O	0.64	0.52	0.65	0.71
K_2O	0.20	0.11	0.23	0.62
TiO_2	0.14	0.17	0.23	0.05
P_2O_5	0.04	0.03	0.03	0.03
Total	99.94	99.07	99.11	100.45
Loss on Ignition 110°C	0.32	0.23	0.32	0.34
Loss on Ignition 1050°C	2.02	1.98	2.07	2.94

Table 12. Hole 453: Trace elements.

Sample (interval in cm)	Sc NAA	Ti XRF	V XRF	Cr XRF	Mn XRF	Fe XRF	Co XRF	Co NAA	Ni XRF	Ni NAA	Zn XRF	Rb XRF
453-53-3, 44-47	383	840	98	88	914	51520	48	55	58	57	14	1.85
453-53-5, 77-88	48	1020	125	103	782	41090	36	38	40	40	7	0.19
453-55-1, 36-48	6.07	1380	188	315		40250	27	31	31	29	4	0.87
453-55-4, 118-123	1.50	300	12	0	875	44240	73	75	25	30	61	3.97

Note: XRF = X-ray fluorescence analysis, NAA = neutron activation analysis.

Table 13. Hole 454: Trace elements (ppm).

Sample (interval in cm)	Sc NAA	Ti XRF	V XRF	Cr XRF	Mn XRF	Fe XRF	Co XRF	Co NAA	Ni XRF	Ni NAA	Zn XRF	Rb XRF	Sr XRF
454-5-1, 38-40	30.6	6000	236	260	968	56840		29		75	54	5.34	176
								31.7		79		5.9	
454-5-3, 52-54	29.1	5760	207	248	867	53900	32		106		42	2.16	1000
								33.9		112		3.2	
454-5-4, 50-52	26.7	4980	186	770	898	61180	48		359		44	1.74	145
								51.9		412			
454-6,CC, 16-18	30	5640	219	270	898	58450	35	36	114		48	0.73	152
										117			
454-8-1, 35-37	29	5340	230	523	883	61390	42		229		50	3.27	146
								44		247			
454-10-1, 58-60	32	6000	265	231	1069	57960	30		76		48	2.98	202
								32.4		84			
454-11-1, 78-80	31	5760	234	223	968	57960	32		109		52	2.40	202
								34		119			
454-11-2, 41-43		6360	265	222	1161	65100	29		57		53	4.39	122
454-12-1, 88-90	30.8	6120	279	218	929	57120	30	31.7	97	103	51	5.56	211
												3.7	
454-14-1, 12-14	30	7380	250	245	1146	62860	32		106		56	7.90	169
								35		127			
454-16-1, 138-141	28.4	6660	257	487	1216	66220	40		223			7.27	164
								42		261			
Average		5964	236										
Dispersion		±670	±20										

Note: XRF = X-ray fluorescence analysis, NAA = neutron activation analysis.

Table 14. Holes 456 and 456A: Trace elements (ppm).

Sample (interval in cm)	Sc NAA	Ti XRF	V XRF	Cr XRF	Mn XRF	Fe XRF	Co XRF	Co NAA	Ni XRF	Ni NAA	Zn XRF	Rb XRF
456A-12-1, 62-64	36	7380	292	219	1224	70840	30		54		47	742
								34		65		
456A-14-1, 25-27	34	6900	247	272	1166	62370	40		84		50	6.13
								42		85		
456-16-2, 98-100	30	7140	290	233	2246	71120	37		74		86	0
								33		72		
456-18-1, 25-27	32	7260	257	335	1286	66640	34		71		56	7.13
								35		73		
456-19-1, 12-15	33	6840	285	314	914	68880	29		44		89	4.46
								29		57		
Average		7635	270									
Dispersion		200	21									

Note: XRF = X-ray fluorescence analysis, NAA = neutron activation analysis.

Table 12. (Continued).

Sr XRF	Y XRF	Zr XRF	Nb XRF	Sb NAA	Cs NAA	Ba NAA	La NAA	Ce NAA	Eu NAA	Tb NAA	Hf NAA	Ta NAA	Tb NAA
316	2.44	814	1.29	0.02		21	0.22	0.3	0.16	0.03	0.11		0.37
286	3.28	6.34	0	0.88	0.02	12	0.11	0.26	0.11	0.09	0.09		0.09
273	3.13	6.93	0.49	0.64		34	0.23		0.13	0.06	0.15		0.13
438	0.36	8.90	0.51	2.02	0.01	230	0.54	0.6	0.08	0.02	0.05		0.31

Table 13. (Continued).

Y XRF	Zr XRF	Nb XRF	Sb NAA	Cs NAA	Ba NAA	La NAA	Ce NAA	Eu NAA	Tb NAA	Hf NAA	Ta NAA	Th NAA	U NAA
29	70	3.09	0.56	0.24	27	2.65	7.4	0.99	0.51	1.63	0.13	0.45	0.19
25	58	3.73	0.14	0.02	31	2.50	6.0	0.93	0.47	1.45	0.11	0.31	0.66
22	54	2.53	0.18	0.02	28	2.33	4.8	0.86	0.44	1.45	0.11	0.51	0.09
26	60	2.38	0.66	0.02	27	3.6	6.9	1.04	0.48	1.52	0.12	0.36	0.1
24	63	4	0.21	0.05	31	3.2	6.8	0.87	0.48	1.5	0.12	0.43	0.07
28	70	4.59	0.83	0.04	19	3.81	8.9	1.12	0.5	1.78	0.15	0.42	0.16
27	68	3.44	0.03			3.83	5.6	1.02	0.5	1.59	0.14	0.74	0.15
29	77	4.25											
29	76	3.62	0.11	0.06	38	2.50	8.0	0.94	0.61	1.62	0.15	0.42	0.13
33	85	3.47	0.06	0.08	20	3.5	8.3	1.21	0.63	2.2	0.17	0.40	0.11
31	82	4.59	0.05	0.03	25	3.51	9.3	1.01	0.59	2.02	0.16	0.39	0.10
27.4 ±3	68.6 ±10	3.54 ±0.75				3.14 ±0.60	7.2 ±1.4	1.00 ±11	0.52 0.67	1.68 ±25	0.14 ±02	0.41 ±06	

Table 14. (Continued).

Sr XRF	Y XRF	Zr XRF	Nb XRF	Sb NAA	Cs NAA	Ba NAA	La NAA	Ce NAA	Eu NAA	Tb NAA	Hf NAA	Ta NAA	Th NAA	U NAA
232	30	72	3.55	0.08	0.17	51	5.05	11.8	1.23	0.66	1.94	0.16	0.69	0.13
174	25	93	3.91	0.06	0.21	13.5	2.99	9.6	1.16	0.60	2.08	0.19	0.29	
146	31	80	347	0.07	0.02	13	2.83	7.6	0.98	0.56	1.82	0.15	0.21	0.05
179	21	86	4.50	0.07	0.33	8	2.99	9.6	1.08	0.58	2.02	0.17	0.22	
172	36	87	3.84	0.09	0.20	11	3.39	8.4	1.15	0.66	2.01	0.16	0.30	0.13
	28.2 ±6	86.5 ±5	3.93 0.43				3.05 0.24	8.8 1	1.09 0.08	0.60 0.04	1.98 0.11	0.17 0.02	0.26 0.05	

Table 15. Hole 458: Trace elements (ppm).

Sample (interval in cm)	Sc NAA	Ti XRF	V XRF	Cr XRF	Mn XRF	Fe XRF	Co XRF	Co NAA	Ni XRF	Ni NAA	Zn XRF	Rb XRF
458-28-1, 102-104		1920	246	250	1069	62230	33		72		67	6.05
458-29-2, 51-54	35	1920	243	227	914	64820	43		68		70	7.38
								43		73		6.5
458-30-2, 32-35	34	1920	196	238	906	63770	37		77		69	10.88
								36		74		9.1
458-32-3, 110-112	32	1620	195	204	867	59080	31		57		35	65.16
								33		65		58
458-33-2, 115-117	34	1740	260	250	929	57960	35		77		39	15.59
								38		76		
458-35-2, 95-98		2040	224	279	813	62300	27		74		49	24.70
458-37-2, 31-35		1800	228	257	852	61460	35		64		42	33.36
458-36-3, 24-27	32	2100	302	286	720	68320	33		71		74	19.82
								31		81		17.3
458-40-1, 116-118	30	2040	199	276	837	71120	39		92		86	14.86
Average		1900	232									
Dispersion		156	35									
458-41-1, 60-63	24	6300	265	233	674	69860	18		14		104	48.56
								18		10		
458-43-1, 88-92		3300	307	257	650	71400	25		73		78	20.04
458-44-1, 54-58	30	3000	281	182	1268	72380	40		72		66	8.73
								39.5		77		7.1
458-47-1, 56-59	30	6060	428	13.17	852	94290	47		32		103	8.50
								45		22		
458-47-2, 34-37	28	5520	399	12.13	697	91840	38		40		101	11.84
								34		22		
458-48-1, 41-43	30	5880	521	20.61	720	94780	42		34		113	10.51
								38		30		9.1

Note: XRF = X-ray fluorescence analysis, NAA = neutron activation analysis.

Table 16. Hole 459B: Trace elements (ppm).

Sample (interval in cm)	Sc NAA	Ti XRF	V XRF	Cr XRF	Mn XRF	Fe XRF	Co XRF	Co NAA	Ni XRF	Ni NAA	Zn XRF	Rb XRF
459B-60-1, 48-51	39	4440	372	299	914	78750	29		40		86	5.65
								30		52		
459B-60-2, 37-90	36	4020	318	152	1053	71400	39		49		55	27.57
								44		55		
459B-61-2, 12-16	35	4200	351	158	1139	72450	38		47		59	10.30
								43		53		
459B-66-2, 92-95	35	6420	419	9.59	1286	88270	40		22		76	13.94
								41.6		24		
459B-69-1, 81-84	28	4680	317	33.39	852	68460	28		26		53	6.17
								29		26		
458B-72-1, 94-97	28	6120	424	14.06	875	84210	34		35		60	36.82
								32		18		
459B-73-2, 13-17	26	6300	329	6.20	929	86590	33		24		114	3.67
								31		18		

Note: XRF = X-ray fluorescence analysis, NAA = neutron activation analysis.

Table 17. Rare earth abundances (ppm) chosen for normalization.

Th[a]	Ta[a]	La	Nb[a]	Ce	Pr	Nd	Zr[a]	Hf[a]	Sm	Ti[a]
0.028	0.031	0.315	0.53	0.81	0.112	0.60	5.13	0.128	0.19	460
Eu	Gd	Tb	Y[a]	Dy	Ho	Er	Tm	Yb	Lu	V[a]
0.072	0.26	0.047	2.16	0.32	0.07	0.21	0.03	0.2	0.032	22

[a] Computed values.

Table 15. (Continued).

Sr XRF	Y XRF	Zr XRF	Nb XRF	Sb NAA	Cs NAA	Ba NAA	La NAA	Ce NAA	Eu NAA	Tb NAA	Tb NAA	Ta NAA	Th NAA	U NAA
100	6.96	35	1.60											
98	4.56	35	1.33	0.12	0.06	16	0.50	1.3	0.28	0.11	0.81	0.05	0.13	
93	5.73	37	1.96	0.07	0.06	12	0.63		0.18	0.10	0.74	0.05	0.14	
95	8.74	30	1.45	0.12	1.02	36	0.80		0.26	0.16	0.80	0.04	0.11	
96	9.32	32	1.04	0.08	0.19	22	0.9	1.4	0.25	0.16	0.8	0.05	0.19	2
121	9.46	38	2.20											
1.5	12.18	33	2.25											
109	8.11	37	2.48	0.13	0.21	15	0.58	2.0	0.29	0.18	0.86	0.06	0.15	0.1
101	5.55	37	2.18	0.15	0.21	16	0.52	2.0	0.20	0.09	0.80	0.06	0.13	0.16
	7.3	35	1.83				0.66	1.68	0.24	0.13	0.80	0.05	0.14	
	2.0	3	0.5				0.16	0.4	0.04	0.04	0.04	0.01	0.03	
159	45.79	92	4.28	0.16	1.03	42	3.68	9.5	1.07	0.70	2.63	0.14	0.26	
141	23.86	53	2.80											
90	12.59	45	0.72	0.08	0.23	16	0.76	1.6	0.28	0.19	1.03	0.05	0.23	
143	30	73	3.25	0.11	0.13	14	2.15	6.1	0.80	0.51	1.72	0.09	0.23	
134	16	61	1.97	0.18	0.22		1.57		0.61	0.29	1.56	0.08	0.20	0.19
136	40	60	3.86	0.13	0.14		2.26	6.1	0.91	0.60	1.44	0.08	0.22	0.10

Table 16. (Continued).

Sr XRF	Y XRF	Zr XRF	Nb XRF	Sb NAA	Cs NAA	Ba NAA	La NAA	Ce NAA	Eu NAA	Tb NAA	Hf NAA	Ta NAA	Th NAA	U NAA
124	22	36	2.95	0.32	0.21	8	2.06	4.6	0.69	0.43	1.16	0.07	0.14	0.09
26	18	41	2.57	0.04	2.8	16	1.20	2.8	0.61	0.36	1.04	0.05	0.11	0.09
113	19	40	2.12	0.03	0.40		1.40	3.5	0.70	0.31	1.10	0.05	0.18	0.10
120	31	62	3.60	0.05	0.39	8	1.88	4.2	0.85	0.58	1.82	0.07	0.19	0.18
142	27	57	2.26	0.12	0.05	15	0.98	5.7	0.64	0.48	1.63	0.06	0.28	0.14
123	30	67	3.69	0.08	1.06	19	2.34	6.4	0.85	0.51	1.75	0.07	0.21	
148	45	82	3.86	0.10	0.11		3.41	8.8	1.02	0.74	2.22	0.09	0.29	0.14